UNIVERSITA' DEGLI STUDI DI VERONA
DIPARTIMENTO MATERNO INFANTILE E DI BIOLOGIA-GENETICA
SEZIONE DI BIOLOGIA E GENETICA

SCUOLA PER IL DOTTORATO IN
SCIENZE BIOMEDICHE TRASLAZIONALI

INDIRIZZO DI
BIOTECNOLOGIE FARMACO-GENETICHE

CICLO XXI

GENE EXPRESSION ANALYSIS OF NON-SYNDROMIC ASCENDING AORTIC ANEURYSMS

S.S.D. BIO/13

Coordinatore: Prof. Guido Francesco Fumagalli

Tutor: Prof. Pier Franco Pignatti

Dottorando: Dott.ssa Alessandra Pasquali

CONTENTS

1. ABSTRACT

The non-syndromic ascending aortic aneurysm is a complex and common disease. Little is known on gene expression and its regulation in aneurysms.

The media coat is principally involved in the disease.

Aim of this study is to identify gene expression differences between aneurysmal and normal ascending aortic media coats.

A total of 41 aneurysmal aortic samples (cases) and 22 aortic samples without aneurysm (controls), has been collected from patients undergoing aneurysmectomy and heart transplantation, respectively.

Gene expression analyses on media coats RNA have been conducted by whole genome microarrays, which detect a total of 21,329 human genes, Real Time PCR, and microRNA microarrays.

Results from whole genome microarrays performed on 3 cases and a pool of 10 controls indicated a total of 17 differentially expressed genes, among which Period homolog 2 (PER2), involved in circadian rhythm, was up-expressed, and Decorin (DCN), involved in remodeling, was down-expressed. The analysis of 4 pool of 3 cases versus a pool of 15 controls confirmed PER2 up-expression. Presently, we validated by Real Time PCR PER2 up-expression and DCN down-expression in aneurysms.

Expression study of a comparison of transcriptomic analysis with proteomic data confirmed up-regulation of 6 genes out of 15 investigated, including NOTCH1 , involved in vascular development.

Expression study of selected genes of NF-kB cascade evidenced a pro-inflammatory status of aneurysmal subjects with bicuspid aortic valve compared to the normal and to tricuspid aortic valve aneurysmal subjects.

Initial microRNA microarray analysis indicates that mir-133, related to NO signaling, may be down-regulated in aneurysms.

In conclusion, genes mainly involved in inflammation and remodeling have been identified with this study. Further expression analyses will better indicate pathways involved in thoracic aortic aneurysms development.

2. INTRODUCTION

The aorta is the major artery which arises from the heart. It carries all the blood that is pumped out of the heart and distributes it via its many branches to all the organs of the body. The aorta is divided into 4 portions: 1) the ascending aorta , 2) the aortic arch 3) the descending thoracic aorta and 4) the abdominal aorta. Aorta's structure is based on three coats, the tunicae intima, media and adventitia, each having specific histologic and functional features that undergo progressive age-related changes.[1,2] Tunica intima, the inner layer, consists of an endothelial lining plus longitudinally oriented connective tissue elements; tunica media, the middle layer, consists of smooth muscle and connective tissue elements arranged in a circular or spiral fashion; and tunica adventitia, the outer layer, consists of connective tissue elements and some smooth muscle cells arranged longitudinally. The vessel is well supplied with nerves (to control the media musculature), blood vessels and lymphatics, distributed largely in the adventitia. The integrity of the layers is disturbed in some individuals by various pathologic processes, the most serious of which increasingly stretches an area of the arterial wall, the so called aneurysm, of which several kinds are known. Aortic aneurysms contribute to the high overall cardiovascular mortality. The incidence of thoracic aortic aneurysms (TAA) is estimated at 6 people per 100.000 per year in Western societies,[3,4] and replacement of the ascending aorta accounts for the majority of thoracic aortic procedures.[5] The mean age at the time of diagnosis ranges from 59 to 69 years.[1] Men are typically diagnosed at a younger age and there is a 2:1 to 4:1 male predominance. Thoracic aneurysms are classified according to one or more aortic segments involved (aortic root, ascending aorta, arch, or descending aorta). Sixty percent of thoracic aortic aneurysms involve the aortic root and/or ascending aorta, 40% involve

the descending aorta. The etiology, natural history, and treatment of thoracic aneurysms differ for each of these segments. The histopathologic abnormality underlying thoracic aortic aneurysms is medial degeneration, traditionally termed cystic medial necrosis, which is characterized by the triad of loss of smooth muscle cells (SMCs), fragmented and diminished number of elastic fibres, and increased accumulation of proteoglycans. Medial degeneration leads to weakening of the aortic wall, which in turn results in aortic dilatation and aneurysm formation. When such aneurysms involve the aortic root, the anatomy is often referred to as annuloaortic ectasia. Cystic medial degeneration occurs normally to some extent with aging, but the process is accelerated by hypertension. All mechanisms that weaken the aortic wall, the aortic lamina media in particular, lead to higher wall stress, which can induce aortic dilatation and aneurysm formation, eventually resulting in aortic dissection or rupture. The occurrence of cystic medial degeneration in young patients is classically associated with Marfan syndrome (or with other less-common connective-tissue disorders, such as Ehlers-Danlos syndrome). The etiopathogenesis of the so called non-syndromic aortic aneurysms, affecting the ascending tract in the absence of atherosclerosis, infection or Marfan's or Ehlers-Danlos' syndrome, is unkown. The extent of genetic heterogeneity is likely to become more evident as more families with thoracic aortic aneurysms are studied. It is also possible that this is actually a polygenic condition, thus explaining the variable expression and penetrance.[6] Moreover, many cases of ascending thoracic aortic aneurysms are associated with an underlying bicuspid aortic valve.[7] Cystic medial degeneration has been found to be the underlying cause of the aortic dilatation associated with a bicuspid aortic valve. In one study, 75% of people with a bicuspid aortic valve undergoing aortic valve replacement surgery had biopsy-proven cystic medial necrosis of the ascending aorta, compared with only 14% of those with tricuspid aortic

valves undergoing similar surgery. Inadequate production of fibrillin-1 during embryogenesis may result in both the bicuspid aortic valve and a weakened aortic wall. Nevertheless, the genetic alteration in these patients with non-syndromic ascending aorta aneurysm is still unknown. The anomalous embryonal valvular genesis and the intrinsic weakness of the aortic wall could be explained by both semilunar valve and main arteries' media coat embryogenetic origin from neural crest. Several assumptions have been proposed to elucidate the progressive aortic wall atrophy in patients with bicuspid aortic valve: smooth muscle cell apoptosis, fibrillin deficiency, increased metalloproteinases secretion. All these conditions could explain extracellular matrix destruction and aortic remodelling.[8,9] For explorative purposes the investigation of a great number of genes by gene expression approaches could be very efficient in outlining transcriptional profiles and molecular pathways involved in the etiopathogenesis of the aortic aneurysm. Microarray technique offers the possibility of comparing transcriptional profiles between pathological and normal tissues. Microarray analysis on genetic specimens from aortic media layer is a precious biotechnological tool that may indicate and localize the genes and the pathways involved in thoracic aortic aneurysms development. Moreover these genes could be analyzed to detect genetic variation causing differential gene expression and possibly involved in aortic aneurysms. Reportedly, proteomic studies can bridge the gaps existing between the results of transcriptional analyses and physiopathological and clinical findings. Proteomic approaches could explain the functional consequences of genetic and transcriptional aberrations. Specific proteins, whose structures, activities, and interactions with other proteins are deeply altered, could be identified as triggers of physiopathologic mechanisms determining the disease's development.[10] A better understanding of the processes underlying the disease may also arise from the study of microRNA. miRNA are sequence-specific

regulators of post-transcriptional gene expression in many eukaryotes. They are believed to control the expression of thousand of target mRNAs, with each mRNA believed to be targeted by multiple microRNAs.[11] However, the function of most microRNAs is not known. The antisense single-stranded microRNAs can bind specific mRNA transcripts through sequences that are significantly, though not completely, complementary to the target mRNA. This process is also known as post-transcriptional gene regulation (PTGS). Some microRNAs can downregulate large numbers of target mRNAs,[12] and it has been speculated that microRNAs could regulate approximately 30% of the human genome.[13] MicroRNAs seem to be responsible for fine regulation of gene expression, ''tuning'' the cellular phenotype during delicate processes like development and differentiation in all organisms, from plants to mammals. A link between microRNAs and human diseases, in particular, has been recently shown. Regulation of gene expression in the mammalian genome, during development, differentiation, and disease, is a complex and multitasked system. To make transcripts instead of proteins is energetically ''less expensive'' for cells and could be the reason why regulation at the RNA level is ''cheaper'' and more efficient than at the protein level. Penetrance in gene expression requires a fine regulation and microRNAs could have a role in different phenotypic expressions of the same gene.

Recent studies have demonstrated that aneurysms associated with bicuspid aortic valve (BAV) exhibit striking histological and molecular differences compared to aneurysms in patients with trileaflet aortic valve (TAV), suggesting that different pathways are responsible for progressive aortic dilatation in these two groups.[14-17] In a study of Collins et al (2003),[18] detailed findings on 111 BAV and TAV aortic ascending aneurysms were described. While the elastic laminae in patients with a BAV remained relatively unfragmented, many cases showed numerous areas in which SMC were lost and the elastic laminae had become collapsed on each

other. SMC loss in patients with a TAV appeared to be associated with collagen deposition. However, no overall difference was observed between TAV and BAV groups with respect to the grade of SMC loss or presence of inflammatory cells. Patients with a TAV did however display more frequent intimal changes than patients with a BAV. LeMaire et al. (2005) [19] found that histological findings in the BAV group were similar to those in control patients; no significant inflammatory infiltrate was seen in either group. Aortas from both the BAV group and control group displayed evenly distributed SMCs throughout the medial lamellae. Aneurysms from TAV patients exhibited severe elastin fragmentation and, compared to both BAV aneurysms and control aortas, markedly decreased elastin staining. Moreover the same paper shown that at the time of aneurysm repair, the pattern of MMP expression and the degree of inflammation differ between aneurysms associated with BAVs and those with TAVs. Histological differences of ascending AA suggest that aneurysms may be the final common manifestation of many different disease processes.

The present study aims to identify genetic factors involved in the non syndromic ascending aortic aneurysm onset, analyzing the gene expression of the tunicae mediae of aortic fragments. To have a framework about which microRNA are implicated in the regulation of the aneurysmal pathology at media layer level, we compared, by microRNA microarray, BAV group, TAV group and female group respect to the male and female groups. Moreover, to investigate if transcriptional differences could delineate the different etiopathogenesis for BAV and TAV ascending aortic aneurysms we studied the gene expression of twelve actors of NF-kB signalling. NF-kB is a largely known nuclear factor initially linked by researchers to the immune response. A growing appreciation for NF-kB as a central mediator of various cardiovascular pathologies has led to the

notion that complete inhibition of this pathway will be beneficial in the setting of vascular stress and heart disease.[20]

The investigation of a great number of genes by the different reported gene expression approaches will be performed in this study for determining agents and metabolic pathways involved in the etiopathogenesis of the ascending aortic aneurysm.

3. MATERIALS AND METHODS

3.1. SAMPLES COLLECTION

In collaboration with the Cardiovascular Surgery Section of the University of Verona, from September 2005 we collected 41 fragments of aneurysmal ascending aorta (cases) and 22 fragments of normal ascending aorta (controls, without aneurysm). The cases came from patients presenting aneurysm not associates to other syndrome (non-syndromic), undergoing aneurysmectomy and the controls came from patients with cardiomyopathy, undergoing heart transplantation for a long-lasting past medical history of congestive heart failure. The clinical features are given for each case and control in the Appendix in Table 1 and in Table 2, respectively: sex, age at surgery and aortic valve type. The case group included 31 males and 10 females, with a mean age of 64; among cases, 14 bicuspid, 26 tricuspid, 1 pentacuspid aortic valve were presented. The control group included 15 males and 7 females, with a mean age of 57; all the controls were with a tricuspid valve. At the time of surgery, after tissue resection, ascending aortic specimens were collected and immediately immersed into RNAlater, a storage solution which prevents the activation of the endogenous RNAses. After 24 hours at 4°C, the samples were stored at -20°C until separation of the coats.

3.2. SAMPLES PREPARATION

Each fragment of the ascending aorta was divided into the three coats (Figure 1) by separation with forceps for dissection and stored in separated tubes with RNAlater at -80°C.

All the expression analysis have been performed on the media layer, the most interesting coat, known as the layer directly involved in the pathology.

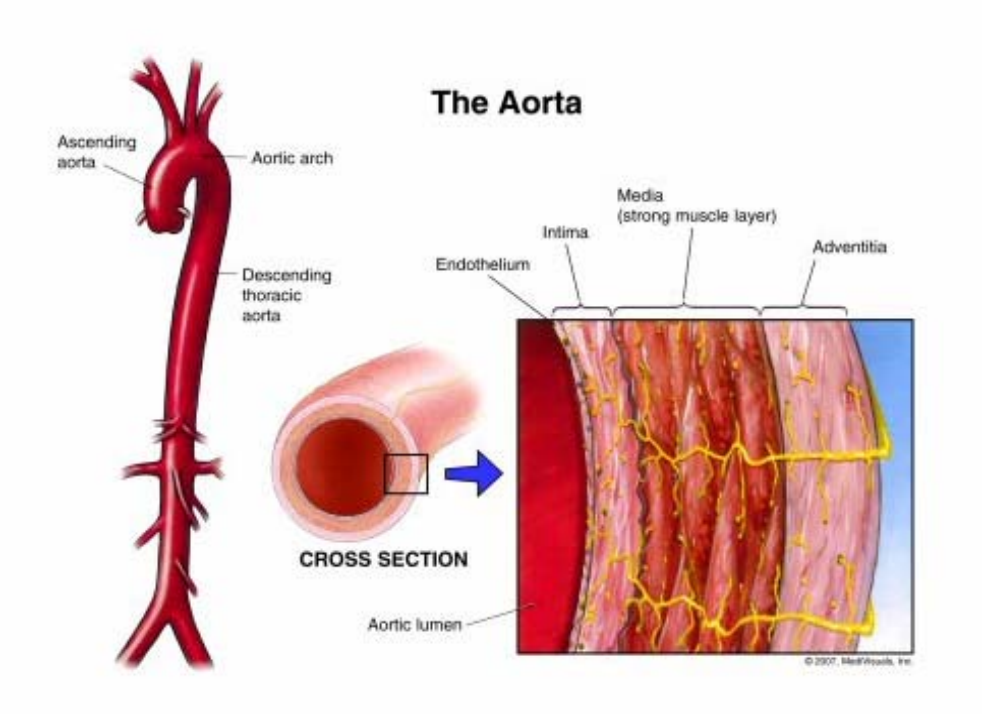

Figure 1. Cross section of the aorta with the three separated layers.

3.3. RNA PREPARATION

3.3.1. RNA extraction

The RNA from all the media coats was extracted by the classical TRIzol® technique to obtain total RNA. TRIzol is a ready-to-use reagent for the isolation of total RNA from cells and tissues. The reagent, a mono-phasic solution of phenol and guanidine isothiocyanate, is an improvement to the single-step RNA isolation method developed by Chomczynski and Sacchi.[21]

For detailed steps see Appendix.

3.3.2. RNA quantification and quality analysis

The extracted RNA was quantified by The Thermo Scientific NanoDrop™ 1000 Spectrophotometer (Celbio) (Figure 2) which enables highly accurate UV/Vis analyses of 1 ul sample with remarkable reproducibility. Pure RNA has a 260/280 Abs ratio of 1.8-2 and a 260/230 Abs ratio of 1.8-2.

A. 

B. 

Figure 2. A. NanoDrop instrument for the quantification of RNA and B. Agilent 2100 BioAnalyzer used to valuate the quality of RNA.

The RNA quality was measured by the use of Agilent 2100 Bioanalyzer instrument (Figure 3). Very small aliquots of total RNAs were loaded into a chip system that contains up to 12 microcapillaries filled with a special matrix for the separation of RNA molecules according to their molecular weight. The chip is loaded into the *Agilent 2100 Bioanalyzer*, an electric field is applied and a short round of electrophoresis produces a complete separation of all the RNA molecules. Capillaries are then scanned by a laser source and two type of results are retrieved:

A) an electropherogram with peaks corresponding to RNA molecules of different molecular weight (28S, 18S, 5S) and whose subtended area is proportional to the abundance of a specific RNA; 28S area should be twice abundant 18S area for the RNA best quality,

B) an image of a virtual agarose gel separation.

The output image is shown in Figure 3.

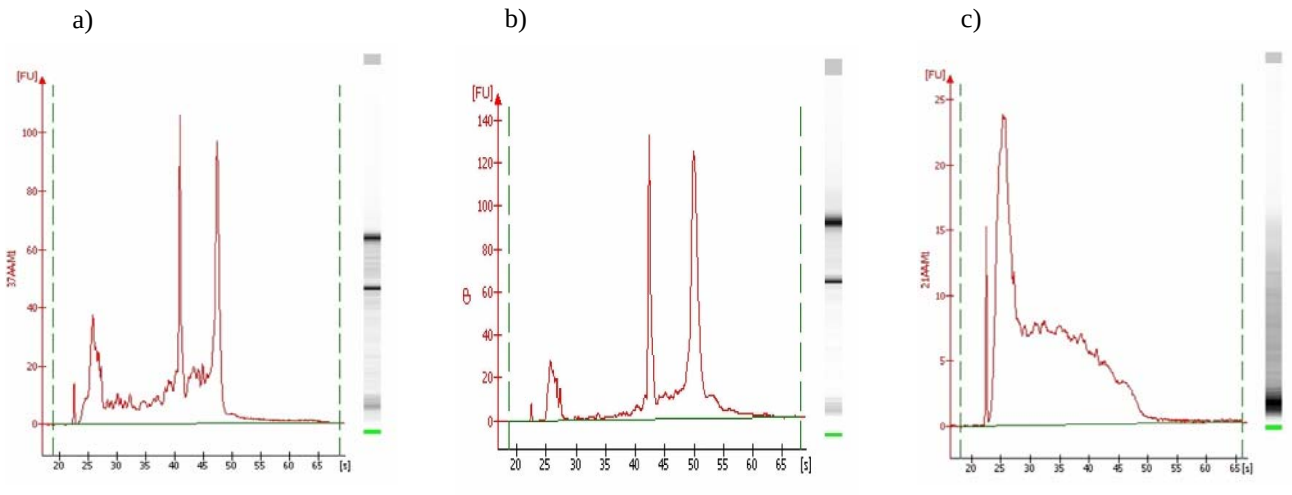

Figure 3. Three Agilent electropherograms indicating a) a quite good, b) good and c) degraded total RNA samples.

3.4. MICROARRAY ANALYSIS

For microarray study we used a platform provided by Microcribi of Padua consisting of 21,329 70mer oligonucleotides. The procedure to hybridize the glass was similar to that cited in our recent paper.[22]

Two types of microarray experiments were conducted:

1- 3 single RNA cases (2 males and 1 female) vs a pool of 10 RNA controls. The cases had a tricuspid aortic valve;

2- 4 pools of 3 RNA cases (all males) each vs a pool of 15 RNA controls. Each case pool was composed of both tricuspid and bicuspid aortic valve samples.

Pooling the RNA controls has the aim to minimize the inter-individual genetic differences and maximize the typical features of the normal tissue. Instead pooling only 3 cases in a sample had the aim to maintain the individually features and characterize a lot of sample simultaneously.

In the same microarray one case (or one pool of cases) and one control pool labeled with different dyes, had to be analyzed in a competitive

hybridization reaction (Figure 4). The *dye-swap,* consisting in the same experiment but with inverted fluorocromes, had been done for each microarray, in order to set the biases led by preferential binding of a fluorophore and by different steric effects of the dyes chemical moieties.
It is important to hybridize a balanced number of picomoles of the two fluorophores: we decided to use 350 pmol for Cy5 and 400 pmol for Cy3, according to different optical characteristics of the two fluorophores.

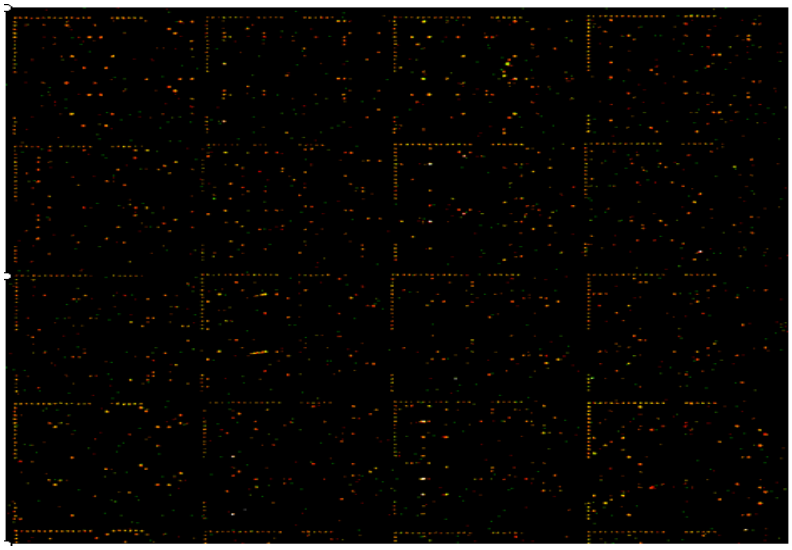

Figure 4. Image of microarray scan in which some subarrays are shown.

RNA amplification and labeling

After quality testing, the RNA had to be amplified and labeled for the following hybridization on a microarray.
To label the target we used the *Amino Allyl MessageAmp™ aRNA amplification* kit (Ambion). The procedure consists of reverse transcription with an oligo(dT) primer bearing a T7 promoter using ArrayScript™, a reverse transcriptase (RT) engineered to produce higher yields of first strand cDNA than wild type enzymes. ArrayScript catalyzes the synthesis of virtually full-length cDNA, which is the best way to ensure production of reproducible microarray samples. The cDNA then undergoes second strand synthesis and clean-up to become a template for in vitro

transcription (IVT) with T7 RNA polymerase. To maximize aRNA yield, the technology is used to generate hundreds to thousands of antisense RNA copies of each mRNA in a sample (In this Protocol the antisense amplified RNA is referred to as aRNA; it is also commonly called cRNA). The IVT is configured to incorporate the modified nucleotide, 5-(3-aminoallyl)-UTP (aaUTP) into the aRNA during in vitro transcription. aaUTP contains a reactive primary amino group on the C5 position of uracil that can be chemically coupled to N-hydroxysuccinimidyl ester-derivatized reactive dyes (NHS ester dyes), such as Cy™3 and Cy5, in a simple, efficient reaction. For each sample we amplified and labeled 1000 ng of RNA. The schematic procedure is represented in Figure 5.

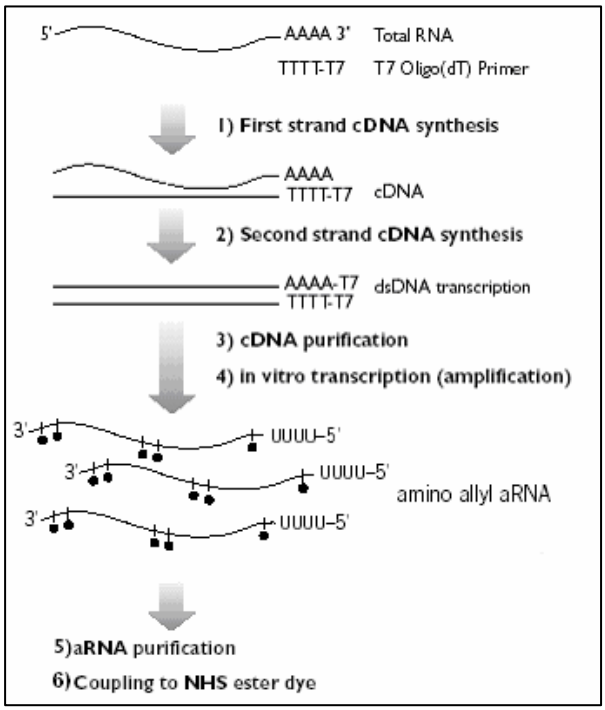

Figure 5. Summary of Amino Allyl MessageAmp II aRNA amplification and labeling procedure

The main steps of RNA amplification and labelling are summarized below (for experimental details see the Appendix).

Reverse Transcription to synthesize first strand cDNA is primed with the T7 Oligo(dT) Primer to synthesize cDNA containing a T7 promoter sequence.
Second Strand cDNA Synthesis converts the single-stranded cDNA into a double-stranded DNA (dsDNA) template for transcription. The reaction employs DNA Polymerase and RNase H to simultaneously degrade the RNA and synthesize second strand cDNA.
cDNA Purification removes RNA, primers, enzymes, and salts that would inhibit in vitro transcription.
In Vitro Transcription to Synthesize Amino Allyl-Modified aRNA with aaUTP generates multiple copies of amino allyl-modified aRNA from the double-stranded cDNA templates; this is the amplification step.
aRNA Purification removes unincorporated NTPs, salts, enzymes, and inorganic phosphate to improve the stability of the aRNA and to facilitate NHS ester coupling or subsequent enzymatic reactions.

The concentration of the aRNA was been determined by measuring its absorbance at 260 nm using *NanoDrop* spectrophotometer.

aRNA: Dye Coupling Reaction takes place between the amino allyl-modified UTP residues on the aRNA and amine reactive Cy3 or Cy5 dyes.
Dye Labeled aRNA Purification removes free dye and exchanges the buffer with Nuclease-free Water.

Then, the absorbance of each sample at both 260 nm (A260) and the maximum absorbance wavelength for the dye used in the coupling reaction (at 550 nm for Cy3 and at 650 nm for Cy5) was measured.

Hybridization of microarray platform

This step consists of pre-hybridization, hybridization and post-hybridization phases.

Pre-hybridization aim to saturate all the sites on the glass area that could unspecific bind the target increasing the background noise.

Hybridization is the crucial step in which the target binds the specific oligonucleotide.

Post-hybridization is a washing step of the slide and removes what is not linked.

For the specific adopted procedure see the Appendix.

3.4.1. Scan of the microarrays

After hybridization, microarray was scanned with ScanArray Lite (PerkinElmer).

It utilizes proven confocal technology, used to accommodate Cyanine-3 and Cyanine-5 fluorescent dyes. The scanner only offers 543 nm and 633 nm excitation wavelengths.

Signal intensity is balanced across all fluorophores in an array by automatically adjusting the laser power or PMT gain to a user defined target of pixel intensity for each fluorophore.

We obtained images from a 5 micrometer resolution producing an accurate fluorescence map. The image file format is TIFF.

3.4.2. Statistical analysis of the microarrays

The fluorescent quantification of the spots was performed by QuantArray software overlapping a GAL file and the normalized results are displayed in a table in CSV format and a scatter plot.

The CSV files were opportunely adjusted for their upload in ExpressConverter software.

Express Converter is a file transformation tool that reads microarray data files in a variety of file formats and generates TIGR MultiExperiment

Viewer file (*.mev*) as output so that the microarray data can be analyzed with MIDAS (Microarray Data Analysis System).

The data can be compared and the normalization is necessary. This critical step can help compensate for variability between slides and fluorescent dyes, as well as other systematic sources of error, by appropriately adjusting the measured array intensities. Normalization modules include locally weighted linear regression (lowess) and total intensity normalization. When the normalization and filtering steps are complete, MIDAS outputs the data in MEV format.

So we have highlighted the differential expressed genes by the coefficient of variation, in order to filter only the very differentially expressed genes. The coefficient of variation describes the magnitude sample values and the variation within them; it is assumed that the values are normally distributed. We adopted a variation of greater or less of 0,5.

$$coefficient\ of\ variation = \frac{standard\ deviation}{mean}$$

The genes, whose quantification was out of the mean line, and with a $\log_{(2)}$ >1 or <-1, were considered differentially expressed in the cases respect to the controls.

3.5. REAL TIME PCR ANALYSIS

Real Time PCR is the continuous collection of fluorescent signal from one or more polymerase chain reaction over a range of cycles. Quantitative real-time PCR is the conversion of the fluorescent signals from each reaction into a numerical value for each sample. We performed two type of chemistries used in real-time PCR: SYBR Green I and TaqMan. The first was used to relatively quantify the genes revealed in the proteomic study and the genes of the NF-kB cascade, whereas the second chemistry was used to relatively quantify the genes resulted from the first microarray

analysis. The experiments are conducted starting from 3 different newly synthesized cDNA to have more statistical power.

SYBR Green I binds to the minor grove of the double-stranded DNA as the double-stranded DNA product is formed. The popularity of SYBR Green I assays is due to three factors: low cost for the dye, ease of assay development (only a pair of primer is required) and the same detection mechanism can be used for every assay.

TaqMan or hydrolysis probes involves a third, fluorescently labeled oligonucleotide, located between the primers, called a probe. The probe has been labeled with a reporter on the 5′ end and a quencher on the 3′ end. A further advantage of a probe-based assay is the avoidance of extraneous signals from primer dimers. When the reporter and quencher dyes are in close proximity in solution, the reporter signal is quenched while when the Taq polymerases ousts the probe the quencher emits fluorescence because no more quenched.

3.5.1. Microarray data confirmation

We performed Taqman Real Time PCR to confirm the differentially expressed genes resulted from the first experiment of microarray. We used the same samples of the microarrays. Each couple of primers were tested by the standard curve. We used 4 housekeeping genes as reference (ACTB, ALDOA, RPS18 and TBP) and valuated them by GeNorm program (http://medgen.ugent.be/~jvdesomp/genorm/).[23] GeNorm is a popular algorithm used to determine the most stable reference (housekeeping) genes from a set of tested candidate reference genes in a given sample panel. From this, a gene expression normalization factor can be calculated for each sample based on the geometric mean of a user-defined number of reference genes.

Then we calculated the normalized relative quantities and then valuated them by a unpaired Student t-test corrected of necessary.

3.5.2. Merging Transcriptomic and Proteomic data

The SYBR Green Real Time PCR was performed to investigate expression profiles of genes coding for the proteins identified by proteomics analysis (prof. Armato, Histology and Embryology Unity, University of Verona) in the same group of samples. Two housekeeping genes were used as reference (GAPDH and TBP) and a normalization factor was calculated by the GeNorm program. The expression profiles of a pool of 7 cases vs a pool of 7 controls were obtained using the same statistical analysis considered above.

3.5.3. NF-kB cascade genes

The nuclear factor-kB (NF-kB) signaling pathway plays a key role in inflammation as in other ways. The principal involved genes in the NF-kB cascade are here valuated by SYBR Green Real-Time PCR: CD14 molecule (CD14), heat shock protein 1 (HSP27), nuclear factor of kappa light polypeptide gene enhancer in B-cells inhibitor, alpha (IKBα), conserved helix-loop-helix ubiquitous kinase (IKBKA), inhibitor of kappa light polypeptide gene enhancer in B-cells, kinase beta (IKBKB), interleukin-1 receptor-associated kinase 4 (IRAK4), myeloid differentiation primary response gene (MD), inhibitor of kappa light polypeptide gene enhancer in B-cells, kinase gamma (NEMO), nuclear factor of kappa light polypeptide gene enhancer in B-cells 1 (P50), transferrin receptor (TFR), toll-like receptor 4 (TLR4), TNF receptor-associated factor 6 (TRAF6).

The experiments were performed on three pools of samples:

- 12 media coat RNAs from male with aneurysm and bicuspid aortic valve,
- 12 media coat RNAs from male with aneurysm and tricuspid aortic valve,
- 12 media coat RNAs from male without aneurysm and with tricuspid aortic valve.

Each sample was individually analysed for every gene expression and the resulting normalized relative quantities have been compared by ANOVA test with post test if necessary.

3.6. MicroRNA ANALYSIS

Twenty-five vials containing samples stabilized in RNAlater were shipped to MACS Myltenyi Biotech on dry ice to test the differentially expressed miRNA by microarray experiments. Each microarray contains 728 human miRNA.

5 pools of 5 RNA each were formed:

- COM: 5 control RNAs from males,
- COF: 5 control RNAs from females,
- ABI: 5 case RNAs from males with bicuspid aortic valve,
- ATRI: 5 case RNAs from males with tricuspid aortic valve,
- AF: 5 case RNAs from females with tricuspid valve.

We tested ABI vs COM, ATRI vs COM, AF vs COF (Table 3). In general, control samples were labeled with Cy3 and case samples were labeled with Cy5.

Experiment n°	Cy3	Cy5	Microarray name
1	COM	ABI	A
2	COM	ATRI	B
3	COF	AF	C

Table 3. Experimental design of the three hybridized microarrays: competitive hybridization of COM and ABI (A), COM and ATRI (B) and COF and AF (C).

RNA was isolated using standard RNA extraction protocols (Trizol), and the quality were checked via the Agilent 2100 Bioanalyzer platform (Agilent Technologies). The fluorescently labeled samples were hybridized overnight to topic defined PIQORTM miRXplore Microarrays using the a-HybTM

Hybridization Station. Fluorescence signals of the hybridized PIQORTM Microarrays were detected using a laser scanner from Agilent (Agilent Technologies). Mean signal and mean local background intensities were obtained for each spot of the microarray images using the ImaGene software (Biodiscovery). Low-quality spots were flagged and excluded from data analysis. Unflagged spots were analysed with the PIQORTM Analyzer software. The PIQORTM Analyzer calculates all normalized mean Cy5/Cy3 ratios of the four replicates per gene.

4. RESULTS

The results described below refer to microarray experiments on aortic aneurysmal subjects vs normal subjects (4.1), to Real-Time PCR experiments to validate selected candidate genes (4.2), and to microRNA study on different subtypes of aneurysmal patients (4.3).

4.1. MICROARRAYS

The statistical analysis of microarray experiments on 3 single cases vs a pool of 10 RNA controls identified 17 differentially expressed genes, listed in Table 4. This relatively small number of genes is due to the stringent analysis performed in order to avoid false positive differentially expressed genes.

GB_accession	Gene_Symbol	Description	LOG_2 MEDIA
NM_001920	DCN	017M24_Decorin	-1.13
NM_030819	MGC11335	010L23_Hypothetical protein MGC11335	1.156
AL080160		046C23_Homo sapiens mRNA	1.054
NM_006871	RIPK3	044D23_Receptor-interacting serine-threonine kinase 3	1.064
NM_006475	OSF-2	035B11_Osteoblast specific factor 2 (fasciclin I-like)	1.028
NM_017805	FLJ20401	041B09_Hypothetical protein FLJ20401	1.025
AF130075		050K09_Homo sapiens clone FLB9413 PRO2532 mRNA, complete cds	1.034
AK027302		054I19_Homo sapiens cDNA FLJ14396 fis, clone HEMBA1003291	1.004
NM_022817	PER2	037B06_Period homolog 2 (Drosophila)	1.033
AB040892	EPHA8	047N18_EphA8	1.029
BC008616		033D05_Homo sapiens, clone IMAGE:4178394, mRNA, partial cds	1.139
AK024599		049L04_Homo sapiens cDNA: FLJ20946 fis, clone ADSE01819	1.167
NM_020979	APS	030H15_Adaptor protein with pleckstrin homology and src homology 2 domains	1.08
NM_018433	LOC55818	048A15_Putative zinc finger protein	1.1
AC004522		041F14_Homo sapiens PAC clone RP4-604G5 from 7q22-q31.1	1.107
NM_020415	FIZZ3	047F14_Found in inflammatory zone 3	1.064
NM_001767	CD2	028M01_CD2 antigen (p50), sheep red blood cell receptor	1.16

Table 4. Seventeen differentially expressed genes in single aneurismal RNAs vs a pool of 10 control RNAs

From the statistical analysis of 4 pools of 3 cases vs a pool of 15 RNA controls, we identified only 2 up-regulated genes: Period homolog 2 (PER2) and Coagulation factor III (F3) (Table 5). This result might be due to the individual inter-variability that can flatten the expression levels.

GB_accession	Gene_Symbol	Description	LOG.MEDIA
NM_022817	PER2	037B06_Period homolog 2 (Drosophila)	1.069
NM_001993	F3	015K04_Coagulation factor III (thromboplastin, tissue factor)	1.020

Table 5. Two differentially expressed genes in 4 pool of aneurismal samples vs a control pool of 15 RNAs.

Based both on the literature and on our microarray results, Decorin and Period homolog 2 genes were firstly selected for further studies by Real Time PCR.

4.2. REAL TIME PCR

4.2.1. Microarray results' confirmation

Validation of the microarray experiments were performed on Period homolog 2 and Decorin genes using the same samples considered in the first microarray analysis. Real Time PCR results confirmed the up-regulation of PER2 with a not very significant p-value (p= 0.0539) and the down-regulation of DCN with a statistically significant p-value (p= 0.0019) (Figure 6).

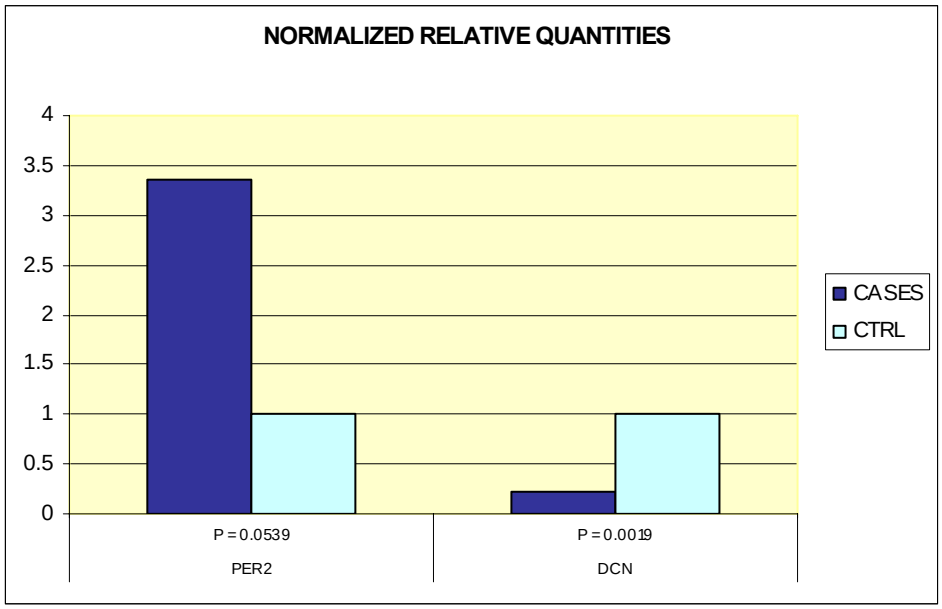

Figure 6. PER2 and DCN gene expression in cases (blue) respect to controls (heavenly).

4.2.2. Proteomic-Transcriptomic analysis

The proteins identified by proteomic study whose genes we analyzed by SYBR Green Real Time PCR are: Jagged1 (JAG1), Follistatin-related protein 1 (FSTL1), Microfibrillar-associated protein 2 (MFAP2), Vimentin (VIM), Testican-2 (SPOCK2), Saposin-A (PSAP), Paxillin (PXN), Leiomodin-3 (LMOD3), Cystathionine gamma-lyase (CTH), Tumor necrosis factor receptor superfamily member 27 (EDA2R), Epiphycan (EPYC), Carbonic anhydrase-related protein (CA8), Glial fibrillary acidic protein (GFAP), and Notch homolog 1, translocation-associated (NOTCH1).

Moreover, Real Time PCR analysis was performed in genes coding for proteins whose levels have been found differentially expressed by the proteomic analysis. Seven aneurismal samples have been compared to seven control samples in this proteomic-genetic study. The results of both proteomic and semiquantitative gene expression analysis are reported in Table 6. Figure 7 shows transcriptomic results.

UniProt	Protein name	Gene name	Proteomic results	Real Time PCR
P78504	Jagged1	JAG1	↑	-
Q12841	Follistatin-related protein 1	FSTL1	↓	-
P55001	Microfibrillar-associated protein 2	MFAP2	↑	↑
P08670	Vimentin	VIM	↓	↑
Q92563	Testican-2	SPOCK2	↑	↑
P07602	Saposin-A	PSAP	↓	-
P49023	Paxillin	PXN	↑	-
Q0VAK6	Leiomodin-3	LMOD3	↑	-
P32929	Cystathionine gamma-lyase	CTH	↑	↑
Q9HAV5	Tumor necrosis factor receptor superfamily member 27	EDA2R	↓	-
Q99645	Epiphycan	EPYC	↑	-
P35219	Carbonic anhydrase-related protein	CA8	↓	-
Q9H382	Fibronectin 1	FN1	↑	↑
P14136	Glial fibrillary acidic protein	GFAP	↑	↑
P46531	Notch homolog 1,translocation-associated	NOTCH1	↑	↑

Table 6. Differentially expression levels of proteins and their coding genes in seven cases compared to seven controls. ↑= up-regulation, ↓= down-regulation, - = no differential expression.

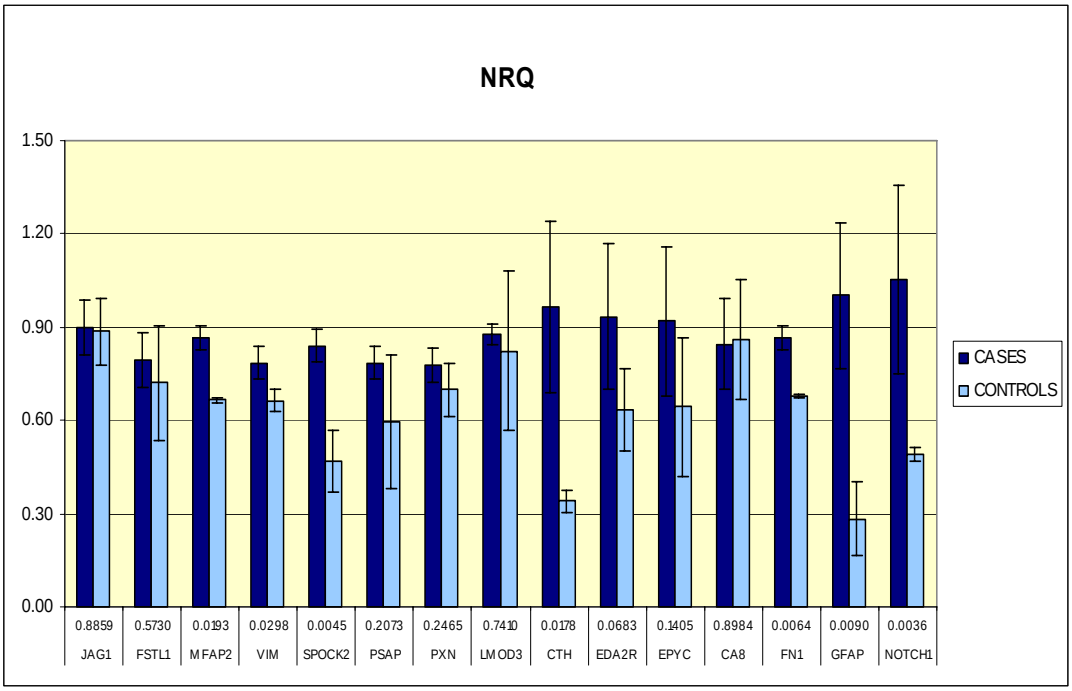

Figure 7. Gene expression levels selected on the basis of proteomic analysis in cases (blue) respect to controls (heavenly). p-value is given below each gene.

JAG1, LMOD3, CA8 genes were not differentially expressed in cases. The data confirm the up-regulation at transcriptional level of MFAP, VIM, SPOCK2, CTH, FN1, GFAP and NOTCH1 genes (p-value<0,05). For the other 5 investigated genes, up-regulation was not statistically significant.

4.2.3. NF-kB pathway analysis

The results of Real Time PCR analysis on twelve selected genes involved in the NF-kB pathway from BAV and TAV cases and from controls are given as normalized relative quantity means in Figure 8. The analysis was conducted on 12 bicuspid aneurysmal samples, 12 control samples and 12 tricuspid aneurysmal samples.

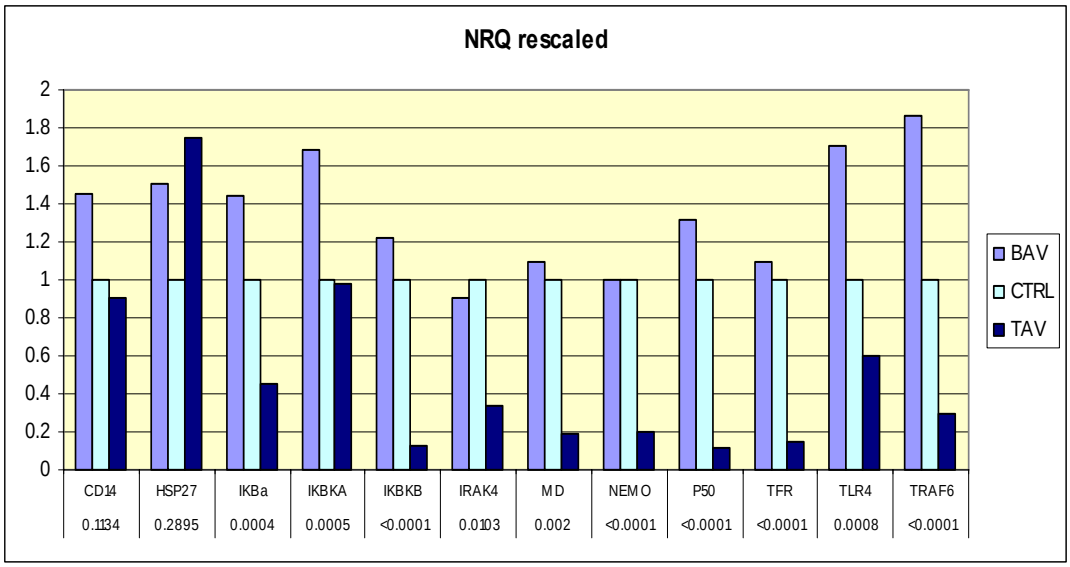

Figure 8. Gene expression profiles of 12 genes involved in NF-kB cascade. The expression levels are reported in BAV (turquoise), Controls CTRL (heavenly), and in TAV (blue) samples for each gene. P-values are shown below the genes.

The general profile of the data indicate that in bicuspid aneurysmal group, the NF-kB involved genes are up-regulated respect to the control group and the tricuspid aneurysmal group resulted down-regulated. Only IRAK4 resulted down-regulated and NEMO was not differentially expressed in bicuspid aneurysmal group. Instead, only HSP27 resulted up-regulated and IKBKA was not differentially expressed in tricuspid aneurysmal group.

After correction for multiple testing, the threshold of statistical significance was set at $P<0.0042$ and significant p-value was obtained in all the genes except CD14, HSP27, and IRAK4.

4.3. miRNA results

microRNA differential expression profile has been analysed in the following three groups: bicuspid aneurysmal males (group A), tricuspid aneurysmal males (group B), and tricuspid aneurysmal females (group C). The miRNAs found down-regulated both in tricuspid aortic valve males and in tricuspid valve females were: mir486-5p, mir133a, mir133b, mir940,

mir125a-3p. The common target genes for all these miRNAs are KCNA1, KLK2, CD47, ARF3, SLC1A2, OCRL, ZNF37A, and CASC4.

The miRNAs found up-regulated both in tricuspid valve males and in tricuspid valve females were: mir15a, mir21, mir25, mir146b-5p, mir29b, mir142-5p, mir422a, mir21*, and mir138-1*. GPR180 is the common target gene for all these miRNAs.

The up-regulated miRNAs in all the three groups were: mir487b and mir128. Several genes are regulated by these two miRNAs: SMAP1, MAP2K4, ZNF831, NTNG1, YWHAB, IDS, CD47, LAPTM-4B, RPS6KB1, CEP350, NRP1, PCF11, USP25, KLHL3, LOC6-43837, NAV1, UNC13C, NAB1, BTB11, SMAD2, RPL10, RCOR1, MUC3B, RNF182, and ZNF664.

Only miRNAs differentially expressed more than 1,5 fold and for at least in two categories have been considered as putative candidate miRNAs and are highlighted by green and red color in Table 7. Green color indicates a <0.66-fold downregulation, corresponding to a fold change <–1.5 of a certain miRNA in comparison to the control sample. Red color indicates a more than 1.5-fold induction of the respective miRNA in comparison to the control.

miRNA name	A	B	C
MIR-486-5P: HSA-MIR-486-5P; MMU-MIR-486	0.717679	0.573901	0.569565
MIR-133A: HSA-MIR-133A; MMU-MIR-133A; RNO-MIR-133A	0.832375	0.562239	0.481803
MIR-133B: HSA-MIR-133B; MMU-MIR-133B; RNO-MIR-133B	0.850565	0.562562	0.5002
MIR-940: HSA-MIR-940		0.478094	0.447289
MIR-125A-3P: HSA-MIR-125A-3P; MMU-MIR-125A-3P; RNO-MIR-125A-3P	0.704419	0.571557	0.473368
MIR-15A: HSA-MIR-15A; MMU-MIR-15A; RNO-MIR-15A	1.094296	3.087589	1.853837
MIR-21: HSA-MIR-21; MMU-MIR-21; RNO-MIR-21	1.131506	4.693228	2.710697
MIR-25: HSA-MIR-25; MMU-MIR-25; RNO-MIR-25		2.798133	1.662063
MIR-146B-5P: HSA-MIR-146B-5P; MMU-MIR-146B; RNO-MIR-146B		3.996174	2.749153
MIR-29B: HSA-MIR-29B; MMU-MIR-29B; RNO-MIR-29B	0.957466	1.741177	1.509631
MIR-142-5P: HSA-MIR-142-5P; MMU-MIR-142-5P; RNO-MIR-142-5P		4.419103	2.69759
MIR-422A: HSA-MIR-422A		2.346378	1.55708
MIR-21*: HSA-MIR-21*		4.208886	2.461323
MIR-138-1*: HSA-MIR-138-1*	1.241529	3.487538	1.818019
MIR-150*: HSA-MIR-150*	2.337072	1.520459	1.394708
MIR-487B: HSA-MIR-487B; MMU-MIR-487B; RNO-MIR-487B	2.045596	1.670535	1.704477
MIR-128: HSA-MIR-128; MMU-MIR-128; RNO-MIR-128	1.824481	4.799245	2.130095

Table 7. miRNA differential expression as $\log_2$ in bicuspid aneurysmal males (A), tricuspid aneurysmal males (B), and tricuspid aneurysmal females. Down- regulated and up-regulated miRNA are indicated in green and red, respectively. microRNAs not highlighted represent those not differentially expressed or those for which there was not microarray data

5. DISCUSSION

Sixty percent of thoracic aortic aneurysms involve the ascending aorta.[24] Research into the pathogenesis of ascending aortic aneurysms is difficult, because this disease is caused by multiple factors, such as hemodynamic, metabolism, inflammation and genetic influences. In addition to activation of proteolysis and inflammation, apoptosis of smooth muscle cells and oxidative stress have been suggested by several clinical-pathological studies, and these factors, together with many others, seem to be intricately interwoven to produce aneurysms. Another difficulty is that suitable animal models are not available for the study of aortic aneurysms. In this respect, the use of a microarray technique with human samples, which can evaluate thousands of genes simultaneously, is of great value and several reports regarding this method in aortic aneurysms have been recently published.[25-27]

The present study is the first one on differential gene expression analysis in media from aorta specimens with and without aneurysm; the media is the most important coat involved in the ascending aortic aneurysms.

Aortic wall thinning and medial smooth muscle cells (SMC) loss is a common finding in aortic wall specimens.[28,29]

In microarray study we took into consideration only patients with tricuspid aortic valve and not many genes were been identified differentially expressed. The results revealed genes involved in morphological and cytoskeletal changes that may lead to the remodeling of aortic wall, while minimal implication of inflammatory pathways seems to be predicted. In particular, until now, we have confirmed the data for two of these.

Decorin (DCN)

One of these is Decorin, small cellular or pericellular matrix proteoglycan that is closely related in structure to biglycan protein. Proteoglycans serve several functions in the artery wall, including regulation of cell adhesion, migration, and proliferation. The major proteoglycan in the arterial ECM synthesized by arterial smooth muscle cells (ASMC) is the large chondroitin sulphate proteoglycan versican, also known as PG-M that can form large aggregates. These large aggregates contribute to tissue mechanical properties, providing a hydrated sponge-like matrix that resists or cushions against deformation. Arteries also contain smaller proteoglycans that contain dermatan sulphate glycosaminoglycans such as decorin and biglycan, which interact with other ECM proteins and with macromolecules that enter the vascular wall such as low density lipoproteins. Not all vascular proteoglycans would be regulated similarly. It has been shown that decorin is specifically decreased by strain. Because decorin binds to collagen[30] and regulates collagen cross-linking,[31] the decrease in decorin could promote disorganization of collagen and a loosening of ECM. Decorin can link LDL and collagen type I in vitro. It is a component of the blood vessel proteoglycans (PG) synthesized by vascular cells, important for collagen assembly and stability. A decrease of decorin in ascending aortic aneurysms vs normal aorta may be the cause for disordered collagen deposition in the aneurysmal wall.[32]

Period homolog 2 (PER2)

Another curious gene resulted from both microarray experiments is Period homolog 2 (PER2), one of the genes involved in the circadian clock rhythm. Daily behavioural and physiological rhythms in mammals are driven by the circadian pacemaker in the suprachiasmatic nucleus (SNC) of the hypothalamus,[33] which orchestrates a hierarchy of molecular clocks in tissues throughout the organism, including heart and vasculature.[34] Peripheral oscillators are synchronized by various neurohumoral stimuli

and food or metabolic cues by several peripheral clocks. One potential function of a peripheral clock is to regenerate a weak or dampened SCN signal, thus amplifying the oscillation of the signal in each tissue. Another is to coordinate locally clock controlled gene expression in each tissue generating an amplified and synchronized rhythm in response to asynchronous blood borne signals.[35] The morning pattern of increased frequency of AAA rupture or aortic dissection resembles that of many other acute cardiovascular diseases, such as acute myocardial infarction,[36] and sudden death.[37] This suggests that common underlying pathophysiologic mechanisms may be responsible for triggering these cardiovascular events. The onset of cardiovascular events is triggered by several pathophysiologic events, in particular, an increase in blood pressure, heart rate, basal vascular tone, vasoconstrictive hormones, which exhibit prominent circadian rhythms with phases that are positively correlated with the timing of excess in cardiovascular events.[38] There are close relationships between blood pressure rhythms and temporal patterns of cardiovascular events.[39] Blood pressure reaches peak values in the morning, although a secondary peak is usually present in the late afternoon or early evening.[40]

It is presumed that such forces act on the aortic wall, which is inherently weakened by genetic and acquired disorders, triggering acute aneurysm rupture or dissection in the early morning hours (Fig 9).[41] As blood pressure undergoes circadian rhythms during the day, it is possible that pressure acts as a synchronizer for peripheral clocks. Thus, chronic pressure overload occurring locally on the heart would be expected to modulate the clock.

Aortic constriction increases the local pressure on the heart, which subsequently maintains cardiac output through the development of hypertrophy. Mechanical stress on cardiomyocytes, caused by increased

blood pressure, for example, induces a cascade of intracellular signaling events resulting in alterations in gene expression.

We found PER2 over-expressed in our microarray study and this could maintain active the cycle resulting in an overloaded blood pressure on the wall.

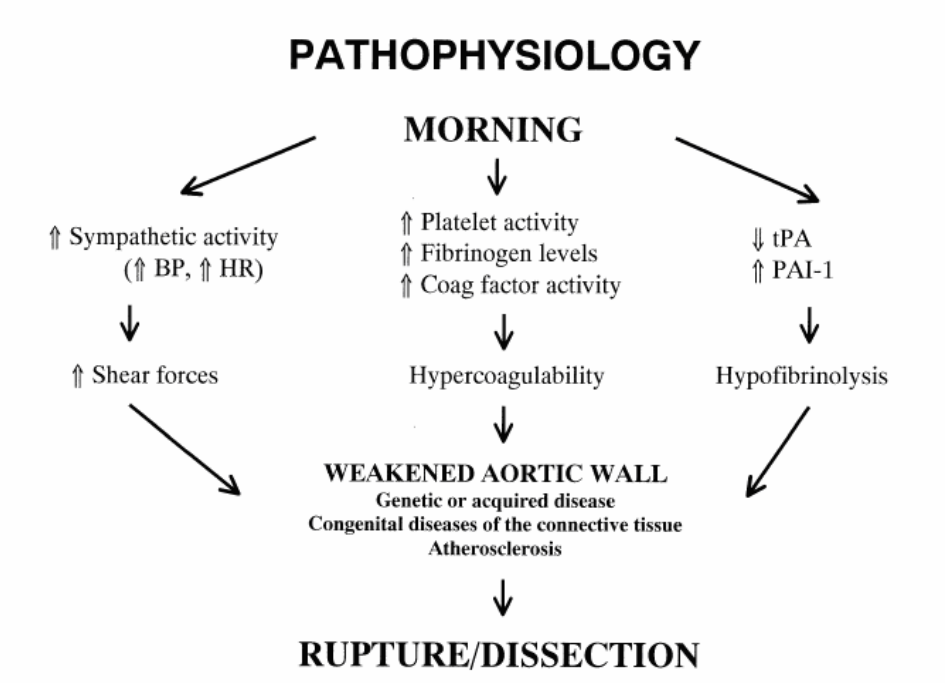

Figure 9. Concurrent pathophysiologic mechanisms underlying circadian variation of aortic rupture or dissection. BP, Blood pressure; HR, heart rate; tPA, tissue plasminogen activator; PAI-1, plasminogen activator inhibitor-1.

Transcriptomics vs Proteomics

Despite the obvious attractions of parallel profiling of transcripts and proteins on a global 'omic' scale, there are practical and biological differences involved in their application. Transcriptomics is now a robust, high-throughput, cost-effective technology capable of simultaneously quantifying tens of thousands of defined mRNA species in a miniaturized, automated format. Conversely, proteomic analysis is currently much more

limited in breadth and depth of coverage owing to variations in protein abundance, hydrophobicity, stability, size and charge. Nevertheless, transcriptomic and proteomic data can be compared and contrasted provided the studies are carefully designed and interpreted. Differential splicing, post-translational modifications and data integration are among some of the future challenges to tackle. Early studies suggested that mRNA levels cannot be consistently relied upon to predict protein abundance.[42,43] On the biological front, differences can result from RNA splicing that is not detectable by the classical microarray platform in use, differential RNA and protein turnover, post-translational modifications, allosteric protein interactions and proteolytic processing events. On the experimental front, challenges in experimental design and data interpretation, as well as technological limitations, contribute to some of the differences observed.[44]

The differential expression levels (up or down) of the genes resulted from the parallel proteomic study have been just in part confirmed with relative quantification of transcripts by Real Time PCR. In some cases we were not able to find the some expression profile for the protein and the corresponding transcripted gene. For example, for JAG1, PXN, LMOD3, and EPYC proteins were up-expressed, instead the transcripts not resulted differentially expressed. FSTL1, PSAP, EDA2R, and CA8 proteins were down-expressed and their genes were not differentially expressed. In the case of VIM, the proteomic (down) and transcriptional (up) profiles were opposite.

Some proteins resulted interesting for the involvement in ascending aortic aneurysms.

NOTCH1 and JAG1

Proteomic study revealed an over-expression of JAG1 protein. This result was not confirmed by Real Time PCR of the corresponding gene

expression, so we decided to evaluate the target receptor of JAG1, NOTCH1. Interestingly, NOTCH1 resulted up-regulated by both proteomic and transcriptomic analysis.

Notch signaling is an extremely conserved and widely used mechanism regulating cell fate in metazoans. Interaction of Notch receptors (Notch) with their ligands (Delta-like or Jagged) leads to cleavage of the Notch intracellular domain (NICD) that migrates into the nucleus. In the nucleus, NICD associates with a transcription factor, RBP-Jk. The NICD-RBP-Jk complex, in turn, up-regulates expression of primary target genes of Notch signaling, such as Jagged1. Recent evidence has demonstrated that the Notch pathway is involved in multiple aspects of vascular development, including proliferation, migration, smooth muscle differentiation, angiogenic processes, and arterial-venous differentiation.[45] Recent findings implicate Notch as playing a critical and non-redundant role in vascular development and maintenance.[46] Lindner et al. found that both smooth muscle cells and endothelial cells of the vasculature greatly increase the expression of these genes in vivo after injury, and that levels of Notch receptor expression may be related to endothelial cell/smooth muscle cell interaction. In general, although Notch1 and Jagged1 and 2 were found expressed at low levels in normal endothelium, there was no expression of Notch2 through 4. All genes were induced after injury, and it is interesting to note that the expression of Notch receptors seemed to be higher in smooth muscle cells in regions of contact with endothelial cells.[47] In our study we found an over expression of both Notch1 and Jagged1 proteins and NOTCH1 gene as an answer to damage vessel. It remains unknown which is the signal that acts like an injury to the aortic wall and if the increased expression of NOTCH1 and JAG1 is a cause or an effect of the signalling.

Cystathionine gamma-lyase (CTH)

Cystathionine gamma-lyase (CTH) is a key enzyme in the trans-sulfuration pathway, which uses L-cysteine to produce hydrogen sulfide (H2S). The CTH/H2S system has been shown to play an important role in regulating cellular functions in different systems. G. Yang et al.[48] found over-expressed CTH in human aorta smooth muscle cells (HASMCs) using a recombinant defective adenovirus containing CTH gene (Ad-CTH). Infection of HASMCs with Ad-CTH resulted in a significant increase in the expression of CTH protein and H2S production. Ad-CTH transfection inhibited cell growth and stimulated apoptosis. CTH is the dominant H2S-generating enzyme in cardiovascular system.[49,50] Consistent with these evidences we found CTH over-expressed at protein and in transcription levels. Abnormal metabolism and functions of endogenous H2S, producted by CTH, may impact on vascular contractile status and structural remodeling of blood vessel walls under different pathophysiological conditions.[51]

Fibronectin1 (FN1)

We found Fibronectin1 (FN1) up-regulated in both transcriptional and proteomic approaches. As reported, Fibronectin is an extracellular matrix protein found only in vertebrate organisms containing endothelium-lined vasculature and is required for cardiovascular development in fish and mice. Fibronectin and its splice variants containing EIIIA and EIIIB domains are highly up-regulated around newly developing vasculature during embryogenesis and in pathological conditions including atherosclerosis, cardiac hypertrophy, and tumorigenesis. Recent genetic studies in fish, frogs and mice have suggested that FN1 functions in maintaining or establishing cell polarity and highlighted the role of FN1 and its splice variants in development of vascular smooth muscle cells.[52] All these differentially expressed genes are involved in morphological and

cytoskeletal changes that may lead to the remodeling and can alter the structural integrity of the aortic wall.

NF-kB

The NF-kB pathway genes resulted up-regulated in BAVs and down-regulated in TAVs respect to controls. The objective of this part of investigation was to compare the patterns of gene expression in aortas between TAV and BAV patients with and the aim to identify markers for ascending aortic aneurysms (AscAAs). Although most AscAAs occur in the presence of a trileaflet aortic valve (TAV), a bicuspid aortic valve (BAV) is a common congenital anomaly associated with an increased risk for an AscAA and dissection independent of functional valve pathology but secondary to inherent structural abnormality of the aorta.[53] MJ Collins et al.[18] found that ascending aortic aneurysms are rarely associated with inflammatory infiltrates in the aortic media of TAV patients. Aortic wall damage in trileaflet aortas develops in several phases and it is both longer standing and more severe than it is in bicuspid aortas (Figure 10). As far as the bicuspid group is concerned, studies indicate that all congenitally bicuspid aortic valves are already morphologically stenotic at birth. Even in the absence of clinical symptoms and of significant pressure gradient, bicuspid valves create turbulence in the ascending aorta which is more than enough to cause aortic wall changes and dilatation.[54]

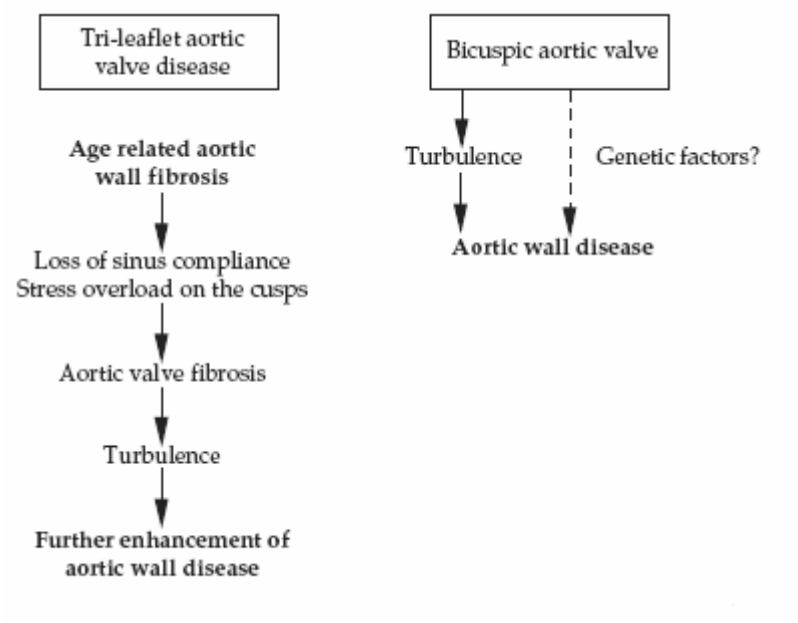

Figure 10. Mechanism of the development of changes in the microstructure of the ascending aorta.

Our findings suggest that the inflammatory response is more activated in BAV ascending aortic aneurysm than in the control group. CD14, HSP27, IKBα, IKBKA, IKBKB, IRAK4, MD, NEMO, P50, TFR, TLR4, TRAF6 genes were up-regulated. Only HSP27 had a inverse profile. In TAV ascending aortic aneurysm group the inflammatory signal was down-regulated respect to the control group and this is consistent with the study of Franz-Xaver Schmid et al.[16] that examined the degree of smooth muscle cell rarefication, leukocyte infiltration, and expression of cell death-initiating proteins at the tissue level in ascending aortic aneurysms of patients with bicuspid and tricuspid aortic valve. The study confirmed that patients with congenitally bicuspid aortic valve have more severe inflammatory as well as degenerative changes in the medial layer than patients with tricuspid aortic valve disease. Although there was no difference in infiltrating leukocyte subsets, patients with a bicuspid aortic valve had fewer numbers of SMCs depicted by a significantly increased apoptotic index for all medial cells, but especially for SMCs. Pathology studies have

clearly demonstrated an association between bicuspid aortic valve and aortic medial abnormalities.[55]

microRNA

Little can be said about microRNA study. We found mir133A and mir133B down-regulated in male and female TAV group. mir133 was found as a key regulator of cardiac hypertrophy and microarray and northern blot analyses revealed that mir-133 is expressed only in the heart and skeletal muscle of human embryos and adults, whereas it is virtually absent from other tissues.[56] One of the target genes of miRNA-133 is CD47. CD47, originally named integrin-associated protein, is a receptor for thrombospondin-1. Recent discovery that thrombospondin-1 acts via CD47 to inhibit nitric oxide signaling throughout the vascular system has given new importance and perhaps a unifying mechanism of action to these enigmatic proteins.[57] Several miRNAs are highly expressed in the hearth and recent data suggest their implication in the control of cardiovascular development and disease as well, raising hope for a new therapy paradign of cardiovascular diseases.[58] In vascular cells, miRNAs have been linked to vasculoproliferative conditions such as angiogenesis and neointimal lesion formation.

Possibilities for diagnostic, prognostic, and therapeutic use of individual miRNAs or miRNA clusters in cardiovascular diseases will have to be further explored.

All these studies revealed genes largely involved in the remodeling, structural integrity and maintenance of the aortic wall.

Future investigations by microarrays will be conducted in order to identify pathways implicated in AscAA, as indicated in our recent paper on atherosclerosis gene expression,[22] in which gene networks were identified.

6. CONCLUSION

The present study considered the non-syndromic ascending aortic aneurysm by different gene expression analysis techniques. Microarray and Real Time PCR studies had revealed genes involved in the structural integrity of aortic vessel, in remodeling and in maintenance of the correct blood flow. A component of inflammation had been found in aneurysmal subjects with bicuspid aortic valve respect to normal and to aneurysmal subjects with tricuspid aortic valve, underlining that the bicuspid valve predisposes to an inflammatory process in the media coat. We identified microRNAs implicated in the disease at media coat level, but is still too early to say their effective involvement in the development of the disease.

This is a study in progress and further analysis will be done. First, the completion of the microarray analysis to all media coat samples could give more informative results about the genes involved in the pathogenesis of the thoracic aortic aneurysm. This will confer a strong statistical power to the study and highlight signaling pathway. Then, gene expression analysis on the intima and media coats could give a more precise localization of the pathology's course.

The integration of the different findings of this research will lead to a deeper understanding of the etiopathogenesis of ascending aortic aneurysm and will be useful in identifying individuals at risk of disease who should be directed towards early detection programs.

7. APPENDIX

7.1. SAMPLE COLLECTION

CONTROLS	sex	Age at surgery	valve type
1C	M	46	tricuspid
2C	M	48	tricuspid
3C	M	50	tricuspid
4C	F	68	tricuspid
5C	F	55	tricuspid
6C	M	56	tricuspid
7C	F	67	tricuspid
8C	M	63	tricuspid
9C	M	53	tricuspid
10C	M	63	tricuspid
11C	M	57	tricuspid
12C	M	61	tricuspid
13C	M	51	tricuspid
14C	M	61	tricuspid
15C	M	58	tricuspid
16C	M	68	tricuspid
17C	M	54	tricuspid
18C	M	67	tricuspid
19C	F	51	tricuspid
20C	F	56	tricuspid
21C	F	40	tricuspid
22C	F	64	tricuspid

Table 1. Clinical features of the control subjects.

CASES	sex	Age at surgery	valve type
1A	M	65	bicuspid
2A	M	65	tricuspid
3A	F	64	tricuspid
4A	M	69	tricuspid
5A	F	71	tricuspid
6A	F	72	tricuspid
7A	M	60	tricuspid
8A	M	43	bicuspid
9A	F	36	tricuspid
10A	F	75	tricuspid
11A	F	74	tricuspid
12A	F	65	bicuspid
13A	M	63	tricuspid
14A	M	66	tricuspid
15A	M	65	bicuspid
16A	M	60	tricuspid
17A	M	62	bicuspid
18A	M	67	bicuspid
19A	M	52	bicuspid
20A	M	44	bicuspid
21A	M	77	bicuspid
22A	M	63	tricuspid
23A	M	38	tricuspid
24A	M	63	tricuspid
25A	M	71	tricuspid
26A	M	53	bicuspid
27A	M	74	tricuspid
28A	M	60	tricuspid
29A	F	75	tricuspid
30A	M	74	tricuspid
31A	F	78	tricuspid
32A	M	63	tricuspid
33A	M	61	bicuspid
34A	M	77	bicuspid
35A	M	62	bicuspid
36A	M	70	tricuspid
37A	M	68	bicuspid
38A	F	74	tricuspid
39A	M	66	tricuspid
40A	M	60	tricuspid
41A	M	44	pentacuspid

Table 2. Clinical features of the case subjects.

7.2. RNA EXTRACTION

The RNA from all the media coats was extracted by the classical TRIzol® technique with the following steps:

- 5 minutes homogenization of TRIzol immersed sample by UltraTurrax 8.0;
- remove insoluble material from the homogenate by centrifugation at 12,000 × *g* for 10 minutes at 2 to 8°C;
- incubate the homogenized samples for 5 minutes at room temperature (RT);
- add 0.2 ml of chloroform per 1 ml of TRIZOL® Reagent;
- shake tubes vigorously by hand for 15 seconds;
- incubate them at RT for 2 to 3 minutes;
- centrifuge the samples at 12,000 × *g* for 15 minutes at 4°C;
- transfer the aqueous phase to a fresh tube;
- add 0.5 ml of isopropyl alcohol per 1 ml of TRIZOL® Reagent;
- incubate samples at RT for 10 minutes;
- centrifuge at 12,000 × *g* for 10 minutes at 4°C (the RNA precipitate, often invisible before centrifugation, forms a gel-like pellet on the side and bottom of the tube.);
- remove the supernatant;
- wash the RNA pellet once with 75% ethanol, adding at least 1 ml of 75% ethanol per 1 ml of TRIZOL® Reagent:
- centrifuge at 7,500 × *g* for 5 minutes at 4°C;
- resuspend the RNA with 15 µl nuclease-free water.

7.3. MICROARRAY EXPERIMENTS

7.3.1. RNA AMPLIFICATION

7.3.1.1. Reverse Transcription to synthesize first strand cDNA

The reverse transcription is primed with the T7 Oligo(dT) Primer to synthesize cDNA containing a T7 promoter sequence.

a. Add to 1000 ng of total RNA 1 µL of T7 Oligo(dT) Primer.

b. Add Nuclease-free Water to a final volume of 12 µL, vortex briefly to mix, then centrifuge to collect the mixture at the bottom of the tube.

c. Incubate 10 min at 70°C in a thermal cycler.

d. Centrifuge samples briefly (~5 sec) to collect them at the bottom of the tube. Place the mixtures on ice.

e. At room temp, prepare Reverse Transcription Master Mix in a nuclease-free tube composed (for a single 20 µL reaction) by:

2 µL 10X First Strand Buffer

4 µL dNTP Mix

1 µL RNase Inhibitor

1 µL ArrayScript

f. Mix well by gently vortexing. Centrifuge briefly (~5 sec) to collect the Reverse Transcription Master Mix at the bottom of the tube and place on ice.

g. Transfer 8 µL of Reverse Transcription Master Mix to each RNA sample. Mix thoroughly by pipetting up and down 2–3 times, then flicking the tube 3–4 times, and centrifuge briefly to collect the reaction in the bottom of the tube.

h. Incubate the samples in a 42°C incubator (we used a water bath) for 2 hr.

i. After the incubation, centrifuge briefly (~5 sec) to collect the reaction at the bottom of the tube.

7.3.1.2. Second Strand cDNA Synthesis

In this step the single-stranded cDNA is converted into a double-stranded DNA (dsDNA) template for transcription. The reaction employs DNA Polymerase and RNase H to simultaneously degrade the RNA and synthesize second strand cDNA.

a. On ice, prepare a Second Strand Master Mix in a nuclease-free tube (for a single 100 µL reaction) in the order listed following:

63 µL Nuclease-free Water

10 µL 10X Second Strand Buffer

4 µL dNTP Mix

2 µL DNA Polymerase

1 µL RNase H

b. Mix well by gently vortexing. Centrifuge briefly (~5 sec) to collect the Second Strand Master Mix at the bottom of the tube and place on ice.

c. Transfer 80 µL of Second Strand Master Mix to each sample. Mix thoroughly by pipetting up and down 2–3 times, then flicking the tube 3–4 times, and centrifuge briefly to collect the reaction in the bottom of the tube.

d. Incubate the tubes for 2 hr in a 16°C water bath.

e. After the 2 hr incubation at 16°C, place the reactions on ice and proceed.

7.3.1.3. cDNA Purification

The purification permits to remove RNA, primers, enzymes, and salts that would inhibit in vitro transcription.

a. Add 250 µL of cDNA Binding Buffer to each sample, and mix thoroughly by pipetting up and down 2–3 times, then flicking the tube 3–4 times. Follow up with a quick spin to collect the reaction in the bottom of the tube. Proceed quickly to the next step.

b. Pipet the cDNA sample\cDNA Binding Buffer (from step 1) onto the center of the cDNA Filter Cartridge.

c. Centrifuge for ~1 min at 10,000 x g, or until the mixture is through the filter.

d. Discard the flow-through and replace the cDNA Filter Cartridge in the wash tube.

e. Apply 500 µL Wash Buffer to each cDNA Filter Cartridge.

f. Centrifuge for ~1 min at 10,000 X g, or until all the Wash Buffer is through the filter.

g. Discard the flow-through and spin the cDNA Filter Cartridge for an additional minute to remove trace amounts of Wash Buffer.

h. Transfer cDNA Filter Cartridge to a cDNA Elution Tube.

i. Apply 9 µL of Nuclease-free Water (preheated to 50–55°C) to the center of the filter in the cDNA Filter Cartridge.

j. Leave at room temperature for 2 min and then centrifuge for ~1.5 min at 10,000 x g, or until all the Nuclease-free Water is through the filter.

k. Elute with a second 9 µL of preheated Nuclease-free Water. The double-stranded cDNA will now be in the eluate (~14 µL).

7.3.1.4. In Vitro Transcription to Synthesize Amino Allyl-Modified aRNA

This is the amplification step and with aaUTP generates multiple copies of amino allyl-modified aRNA from the double-stranded cDNA templates.

a. At room temp, assemble the IVT Master Mix at room temp in the order shown (for a single 40 µL reaction):

3 µL aaUTP (50 mM)

12 µL ATP, CTP, GTP Mix (25 mM)

3 µL UTP Solution (50 mM)

4 µL T7 10X Reaction Buffer

4 µL T7 Enzyme Mix

b. Mix well by gently vortexing. Centrifuge briefly (~5 sec) to collect the IVT Master Mix at the bottom of the tube and place on ice.

c. Transfer 26 µL of IVT Master Mix to each sample. Mix thoroughly by pipetting up and down 2–3 times, then flicking the tube 3–4 times, and centrifuge briefly to collect the reaction in the bottom of the tube.

d. Once assembled, incubate the tubes for 14 hr at 37°C in the water bath.

e. Stop the reaction by adding 60 µL Nuclease-free Water to each aRNA sample to bring the final volume to 100 µL. Mix thoroughly by gentle vortexing.

Proceed to the aRNA purification.

7.3.1.5. aRNA Purification

This purification removes unincorporated aaUTP and Tris from IVT reactions that would otherwise compete with the aRNA for dye coupling; it also removes enzymes, salts, and other unincorporated nucleotides to improve the stability of the aRNA.

Preheat Nuclease-free Water to 50–60°C

a. Check to make sure that each IVT reaction was brought to 100 µL with Nuclease-free Water.

b. Add 350 µL of aRNA Binding Buffer to each aRNA sample. Proceed to the next step immediately.

c. Add 250 µL of ACS grade 100% ethanol to each aRNA sample, and mix by pipetting the mixture up and down 3 times. Proceed immediately to the next step as soon as you have mixed the ethanol into each sample. Any delay in proceeding could result in loss of

aRNA because once the ethanol is added, the aRNA will be in a semiprecipitated state.

d. Pipet each sample mixture onto the center of the filter in the aRNA Filter Cartridge.

e. Centrifuge for ~1 min at 10,000 X g. Continue until the mixture has passed through the filter.

f. Discard the flow-through and replace the aRNA Filter Cartridge back into the aRNA Collection Tube.

g. Apply 650 µL Wash Buffer to each aRNA Filter Cartridge.

h. Centrifuge for ~1 min at 10,000 X g, or until all the Wash Buffer is through the filter.

i. Discard the flow-through and spin the aRNA Filter Cartridge for an additional ~1 min to remove trace amounts of Wash Buffer.

j. Transfer Filter Cartridge(s) to a fresh aRNA Collection Tube.

k. To the center of the filter, add 70 µL Nuclease-free Water (preheated to 50–60°C).

l. Leave at room temp for 2 min and then centrifuge for ~1.5 min at 10,000 X g, or until the Nuclease-free Water is through the filter.

m. Repeat the steps j-k.

n. The aRNA will now be in the aRNA Collection Tube in 140 µL of Nuclease-free Water.

Store purified aRNA at –80°C.

The concentration of the aRNA was been determined by measuring its absorbance at 260 nm using *NanoDrop* spectrophotometer.

7.3.2. RNA LABELING

7.3.2.1. aRNA:Dye Coupling Reaction

The Dye takes place between the amino allyl-modified UTP residues on the aRNA and amine reactive Cy3 or Cy5 dyes.

The steps are indicated following.

a. Add 11 µL of DMSO to one tube of Cy3 or Cy5 reactive dye, and vortex to mix thoroughly.

b. Keep the resuspended dye in the dark at room temperature for up to 1 hr until you are ready to use it.

c. Vacuum dry on medium 5 µg of amino allyl-modified aRNA until no liquid remains.

d. To the dried amino allyl aRNA (5 µg), add 9 µL Coupling Buffer and resuspend thoroughly by vortexing gently.

e. Add 11 µL of prepared dye (from step a) to the aRNA:Coupling Buffer mixture. Mix well by vortexing gently.

f. 60 min incubation at room temp allows the dye coupling reaction to occur.

g. To quench the reaction, add 4.5 µL 4M Hydroxylamine and mix well by vortexing gently.

h. Incubate the reaction in the dark at room temp for 15 min. (During this incubation, the large molar excess of hydroxylamine will quench the amine-reactive groups on the unreacted dye molecules.)

i. Add 5.5 µL Nuclease-free Water to each sample to bring the volume to 30 µL.

7.3.2.2. Dye Labeled aRNA Purification

This purification removes excess dye from the labeled aRNA and exchanges the

buffer with Nuclease-free Water.

Before beginning the labeled aRNA purification, preheat the bottle of Nuclease-free Water to 50–60°C for at least 10 min.

a. Add 105 µL of aRNA Binding Buffer to each aRNA sample. Proceed to the next step immediately.

b. Add 75 µL of ACS grade 100% ethanol to each labeled aRNA sample, and mix by pipetting the mixture up and down 3 times. Proceed immediately to the next step as soon as you have mixed the ethanol into

each sample. Any delay in proceeding could result in loss of aRNA because once the ethanol is added, the aRNA will be in a semiprecipitated state.

c. Pipet each sample mixture onto the center of the filter in the Labeled aRNA Filter Cartridge.

d. Centrifuge for ~1 min at 10,000 X g. Continue until the mixture has passed through the filter.

e. Discard the flow-through and replace the Labeled aRNA Filter Cartridge back into the Labeled aRNA Collection Tube.

f. Apply 500 µL Wash Buffer to each Labeled aRNA Filter Cartridge.

g. Centrifuge for ~1 min at 10,000 X g, or until all the Wash Buffer passes through the filter.

h. Discard the flow-through and centrifuge for an additional ~1 min to remove trace amounts of Wash Buffer.

i. Transfer the Labeled aRNA Filter Cartridge to a Labeled aRNA Elution Tube.

j. To the center of the filter, add 20 µL Nuclease-free Water that is preheated to 50–60°C.

k. Leave at room temp for 2 min and then centrifuge for ~1.5 min at 10,000 X g, or until the Nuclease-free Water is through the filter.

l. Repeat steps j-k three times with 20 µL each of preheated Nuclease-free Water.

m. The aRNA will now be in the Labeled aRNA Elution Tube in ~60 µL of Nuclease-free Water.

n. Determine the aRNA concentration using *NanoDrop.* Measure the absorbance of each sample at 260 nm (A260) and also at the maximum absorbance wavelength for the dye used in the coupling reaction.

The absorbance for Cy3 is at 550 nm and for Cy5 at 650 nm.

7.3.3. HYBRIDIZATION ON MICROARRAY PLATFORMS

7.3.3.1. Pre-hybridization

A pre-hybridization buffer is composed by: SSC 20X with final concentration of 5X, SDS 10% with final concentration of 0,1%, ssDNA with final concentration 100 ng/µl, Denhardt's solution 50X with final concentration 5X and milliQ water to volume.

About 80 µl of pre-hybridization buffer, preheat at 48°C, are pipetted on the glass. A cover glass is applied above and then the glass is positioned in a hybridization chamber (HybChamber of GeneMachines) with about 100 µl of SSC 3X to avoid the evaporation of the buffer, then the formation of crystals.

Incubate the prepared chamber in a water bath at 42°C for at least 4 hours.

After the pre-hybridization, the glass had to be washed and then dried by centrifugation at room temperature at 1000 rpm for 1 minute.

In Figure 11 is shown the used pre-hybridization chamber.

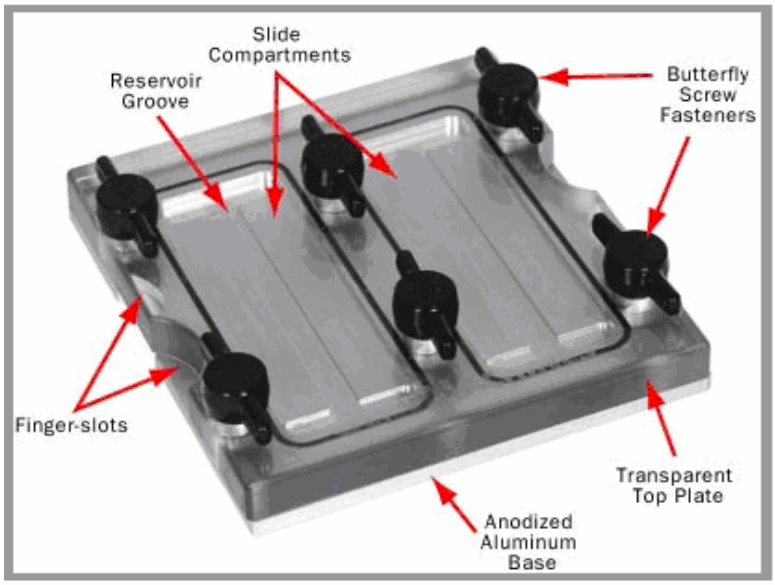

Figure 11. Designed specifically for post-process microarraying, the HybChambers are easier to use than any other hybridization chambers on the market.

7.3.3.2. Hybridization

Once pre-hybridizated, the glass is ready for the hybridization.

The two labelled aRNA are put together and then washed and precipitated:

- Add the 4/5 of the total volume in ammonium acetate
- Add to the obtained volume 2,5 times of EtOH 100%
- Put at -20°C for at least 2 hr
- Centrifugate at 13000 g for 20 min at 4°C
- Throw away the supernatant and keep the pellet
- Wash with 500 µl EtOH 75%
- Centrifugate at 13000 g for 12 min at 4°C
- Throw away the supernatant and keep the pellet
- Second wash with 300 µl EtOH 75%
- Centrifugate at 13000 g for 16 min at 4°C
- Throw away the supernatant
- Keep in the dark

Preheat the hybridization buffer at 48°C

The hybridization buffer is composed by SSC 20X with final concentration of 5X, SDS 10% with final concentration of 0,1%, formamide final concentration 50% and milliQ water to volume.

Dissolve the pellet in 10 µl of DEPC-treated Water and add 110 µl of hybridization buffer.

Denature the sample at 65°C for 1 minute.

The 120 µl sample is pipetted on the glass. A cover glass is applied above and then the glass is positioned in the hybridization chamber (HybChamber of GeneMachines).

Incubate the prepared chamber in a water bath at 42°C for 40 hours.

7.3.3.3. Post-hybridization

The glass had to be washed with:

1X SSC 0,1% SDS for 5 minutes

0,2X SSC 0,1% SDS for 5 minutes

0,2X SSC for 5 minutes

0,1X SSC for 2 minutes

Then we could proceed with the scan of the microarray.

8. ABBREVIATIONS

TAA = thoracic aortic aneurysm

SMC = smooth muscle cell

PTGS = post-transcriptional gene regulation

BAV = bicuspid aortic valve

TAV = tricuspid aortic valve

ECM = extracellular matrix

ASMC = arterial smooth muscle cell

SCN = suprachiasmatic nucleus

AscAA = ascending aortic aneurysm

NRQ = normalized relative quantities

9. REFERENCES

1. Coady MA, Rizzo JA, Goldstein LJ, Elefteriades JA. Natural history, pathogenesis, and etiology of thoracic aortic aneurysms and dissections. Cardiol Clin. 1999 Nov;17(4):615-35.

2. Spina M, Garbisa S, Hinnie J, Hunter JC, Serafini-Fracassini A. Age-related changes in composition and mechanical properties of the tunica media of the upper thoracic human aorta. Arteriosclerosis. 1983 Jan-Feb;3(1):64-76.

3. Ince H, Nienaber CA. Etiology, pathogenesis and management of thoracic aortic aneurysm. Nat Clin Pract Cardiovasc Med. 2007 Aug;4(8):418-27.

4. Bickerstaff LK, Pairolero PC, Hollier LH, Melton LJ, Van Peenen HJ, Cherry KJ, Joyce JW, Lie JT. Thoracic aortic aneurysms: a population-based study. Surgery. 1982 Dec;92(6):1103-8.

5. Gillum RF. Epidemiology of aortic aneurysm in the United States. J Clin Epidemiol. 1995 Nov;48(11):1289-98.

6. Milewicz DM, Chen H, Park ES, Petty EM, Zaghi H, Shashidhar G, Willing M, Patel V. Reduced penetrance and variable expressivity of familial thoracic aortic aneurysms/dissections. Am J Cardiol. 1998 Aug 15;82(4):474-9.

7. Feindel CM, David TE. Aortic valve sparing operations: basic concepts. Int J Cardiol. 2004 Dec;97 Suppl 1:61-6.

8. Ikonomidis JS, Jones JA, Barbour JR, Stroud RE, Clark LL, Kaplan BS, Zeeshan A, Bavaria JE, Gorman JH 3rd, Spinale FG, Gorman RC. Expression of matrix metalloproteinases and endogenous inhibitors within ascending aortic aneurysms of patients with bicuspid or tricuspid aortic valves. J Thorac Cardiovasc Surg. 2007 Apr;133(4):1028-36. Epub 2007 Feb 26.

9. Matt P, Carrel T, White M, Lefkovits I, Van Eyk J. Proteomics in cardiovascular surgery. J Thorac Cardiovasc Surg. 2007 Jan;133(1):210-4.

10. Zerkowski HR, Grussenmeyer T, Matt P, Grapow M, Engelhardt S, Lefkovits I. Proteomics strategies in cardiovascular research. J Proteome Res. 2004 Mar-Apr;3(2):200-8.

11. Sevignani C, Calin GA, Siracusa LD, Croce CM. Mammalian microRNAs: a small world for fine-tuning gene expression. Mamm Genome. 2006 Mar;17(3):189-202. Epub 2006 Mar 3.

12. Lim LP, Lau NC, Garrett-Engele P, Grimson A, Schelter JM, Castle J, Bartel DP, Linsley PS, Johnson JM. Microarray analysis shows that some microRNAs downregulate large numbers of target mRNAs. Nature. 2005 Feb 17;433(7027):769-73. Epub 2005 Jan 30.

13. Bartel DP. MicroRNAs: genomics, biogenesis, mechanism, and function. Cell. 2004 Jan 23;116(2):281-97.

14. Bonderman D, Gharehbaghi-Schnell E, Wollenek G, Maurer G, Baumgartner H, Lang IM. Mechanisms underlying aortic dilatation in congenital aortic valve malformation. Circulation 99: 2138, 1999.

15. Fedak P. W, de Sa MP, Verma S, Nili N, Kazemian P, Butany J, Strauss BH, Weisel RD, David TE. Vascular matrix remodeling in patients with bicuspid aortic valve malformations: Implications for aortic dilatation. J. Thorac. Cardiovasc. Surg. 126: 797, 2003.

16. Schmid FX, Bielenberg K, Schneider A, Haussler A, Keyser A, Birnbaum D. Ascending aortic aneurysm associated with bicuspid and tricuspid aortic valve: Involvement and clinical relevance of smooth muscle cell apoptosis and expression of cell death-initiating proteins. Eur. J. Cardiothorac. Surg. 23: 537, 2003.

17. Boyum J, Fellinger EK, Schmoker JD, Trombley L, McPartland K, Ittleman FP, Howard AB. Matrix metalloproteinase activity in thoracic aortic aneurysms associated with bicuspid and tricuspid aortic valves. J. Thorac. Cardiovasc. Surg. 127: 686, 2004.

18. Collins MJ, Dev V, Strauss BH, Fedak PW, Butany J. Variation in the histopathological features of patients with ascending aortic aneurysms: a study of 111 surgically excised cases. J Clin Pathol. 2008 Apr;61(4):519-23. Epub 2007 Oct 15.

19. LeMaire SA, Wang X, Wilks JA, Carter SA, Wen S, Won T, Leonardelli D, Anand G, Conklin LD, Wang XL, Thompson RW, Coselli JS. Matrix metalloproteinases in ascending aortic

aneurysms: bicuspid versus trileaflet aortic valves. J Surg Res. 2005 Jan;123(1):40-8.

20. Hall G, Hasday JD, Rogers TB Regulating the regulator: NF-kB signaling in the heart. J Mol Cell Cardiol 41 (2006) 580-591.

21. Chomczynski P, Sacchi N. Single-step method of RNA isolation by acid guanidinium thiocyanate-phenol-chloroform extraction. Anal Biochem. 1987 Apr;162(1):156-9.

22. Cagnin S, Biscuola M, Patuzzo C, Trabetti E, Pasquali A, Laveder P, Faggian G, Iafrancesco M, Mazzucco A, Pignatti PF, Lanfranchi G. Reconstruction and functional analysis of altered molecular pathways in human atherosclerotic arteries. BMC Genomics. 2009 Jan 9;10(1):13.

23. Vandesompele J, De Preter K, Pattyn F, Poppe B, Van Roy N, De Paepe A, Speleman F. Accurate normalization of real-time quantitative RT-PCR data by geometric averaging of multiple internal control genes. Genome Biol. 2002 Jun 18;3(7):RESEARCH0034. Epub 2002 Jun 18.

24. Isselbacher EM. Thoracic and abdominal aortic aneurysms. Circulation. 2005 Feb 15;111(6):816-28.

25. Koullias GJ, Ravichandran P, Korkolis DP, Rimm DL, Elefteriades JA. Increased tissue microarray matrix metalloproteinase expression favors proteolysis in thoracic aortic aneurysms and dissections. Ann Thorac Surg. 2004 Dec;78(6):2106-10; discussion 2110-1.

26. Absi TS, Sundt TM 3rd, Tung WS, Moon M, Lee JK, Damiano RR Jr, Thompson RW. Altered patterns of gene expression distinguishing ascending aortic aneurysms from abdominal aortic aneurysms: complementary DNA expression profiling in the molecular characterization of aortic disease. J Thorac Cardiovasc Surg. 2003 Aug;126(2):344-57; discission 357.

27. Taketani T, Imai Y, Morota T, Maemura K, Morita H, Hayashi D, Yamazaki T, Nagai R, Takamoto S. Altered patterns of gene expression specific to thoracic aortic aneurysms: microarray

analysis of surgically resected specimens. Int Heart J. 2005 Mar;46(2):265-77.

28. Klima T, Spjut HJ, Coelho A, Gray AG, Wukasch DC, Reul GJ Jr, Cooley DA. The morphology of ascending aortic aneurysms. Hum Pathol. 1983 Sep;14(9):810-7.

29. Savunen T, Aho HJ. Annulo-aortic ectasia. Light and electron microscopic changes in aortic media. Virchows Arch A Pathol Anat Histopathol. 1985;407(3):279-88.

30. Keene DR, San Antonio JD, Mayne R, McQuillan DJ, Sarris G, Santoro SA, Iozzo RV. Decorin binds near the C terminus of type I collagen. J Biol Chem. 2000 Jul 21;275(29):21801-4.

31. Danielson KG, Baribault H, Holmes DF, Graham H, Kadler KE, Iozzo RV. Targeted disruption of decorin leads to abnormal collagen fibril morphology and skin fragility. J Cell Biol. 1997 Feb 10;136(3):729-43.

32. Pentikäinen MO, Oörni K, Lassila R, Kovanen PT. The proteoglycan decorin links low density lipoproteins with collagen type I. J Biol Chem. 1997 Mar 21;272(12):7633-8.

33. Ralph MR, Foster RG, Davis FC, Menaker M. Transplanted suprachiasmatic nucleus determines circadian period. Science. 1990 Feb 23;247(4945):975-8.

34. Martino TA, Tata N, Belsham DD, Chalmers J, Straume M, Lee P, Pribiag H, Khaper N, Liu PP, Dawood F, Backx PH, Ralph MR, Sole MJ. Disturbed diurnal rhythm alters gene expression and exacerbates cardiovascular disease with rescue by resynchronization. Hypertension. 2007 May;49(5):1104-13. Epub 2007 Mar 5.

35. Reilly DF, Westgate EJ, FitzGerald GA. Peripheral circadian clocks in the vasculature. Arterioscler Thromb Vasc Biol. 2007 Aug;27(8):1694-705. Epub 2007 May 31.

36. Muller JE, Stone PH, Turi ZG, Rutherford JD, Czeisler CA, Parker C, Poole WK, Passamani E, Roberts R, Robertson T, et al. Circadian variation in the frequency of onset of acute myocardial infarction. N Engl J Med. 1985 Nov 21;313(21):1315-22.

37. Muller JE, Ludmer PL, Willich SN, Tofler GH, Aylmer G, Klangos I, Stone PH. Circadian variation in the frequency of sudden cardiac death. Circulation. 1987 Jan;75(1):131-8.

38. Portaluppi F, Manfredini R, Fersini C. From a static to a dynamic concept of risk: the circadian epidemiology of cardiovascular events. Chronobiol Int. 1999 Jan;16(1):33-49.

39. Manfredini R, Gallerani M, Portaluppi F, Fersini C. Relationships of the circadian rhythms of thrombotic, ischemic, hemorrhagic, and arrhythmic events to blood pressure rhythms. Ann N Y Acad Sci. 1996 Aug 15;783:141-58.

40. Millar-Craig MW, Bishop CN, Raftery EB. Circadian variation of blood-pressure. Lancet. 1978 Apr 15;1(8068):795-7.

41. Manfredini R, Boari B, Gallerani M, Salmi R, Bossone E, Distante A, Eagle KA, Mehta RH. Chronobiology of rupture and dissection of aortic aneurysms. J Vasc Surg. 2004 Aug;40(2):382-8.

42. Anderson L, Seilhamer J. A comparison of selected mRNA and protein abundances in human liver. Electrophoresis. 1997 Mar-Apr;18(3-4):533-7.

43. Gygi SP, Rochon Y, Franza BR, Aebersold R. Correlation between protein and mRNA abundance in yeast. Mol Cell Biol. 1999 Mar;19(3):1720-30.

44. Hegde PS, White IR, Debouck C. Interplay of transcriptomics and proteomics. Curr Opin Biotechnol. 2003 Dec;14(6):647-51.

45. Iso T, Hamamori Y, Kedes L. Notch signaling in vascular development. Arterioscler Thromb Vasc Biol. 2003 Apr 1;23(4):543-53. Epub 2003 Feb 13.

46. Karsan A. The role of notch in modeling and maintaining the vasculature. Can J Physiol Pharmacol. 2005 Jan;83(1):14-23.

47. Lindner V, Booth C, Prudovsky I, Small D, Maciag T, Liaw L. Members of the Jagged/Notch gene families are expressed in injured arteries and regulate cell phenotype via alterations in cell matrix and cell-cell interaction. Am J Pathol. 2001 Sep;159(3):875-83.

48. Yang G, Wu L, Wang R. Pro-apoptotic effect of endogenous H2S on human aorta smooth muscle cells. FASEB J. 2006 Mar;20(3):553-5. Epub 2006 Jan 17.

49. Zhao W, Zhang J, Lu Y, Wang R. The vasorelaxant effect of H(2)S as a novel endogenous gaseous K(ATP) channel opener. EMBO J. 2001 Nov 1;20(21):6008-16.

50. Zhao W, Wang R. H(2)S-induced vasorelaxation and underlying cellular and molecular mechanisms. Am J Physiol Heart Circ Physiol. 2002 Aug;283(2):H474-80.

51. Wang R. Two's company, three's a crowd: can H2S be the third endogenous gaseous transmitter? FASEB J. 2002 Nov;16(13):1792-8.

52. Astrof S, Hynes RO. Fibronectins in vascular morphogenesis. Angiogenesis. 2009 Feb 14. [Epub ahead of print]

53. Majumdar R, Miller DV, Ballman KV, Unnikrishnan G, McKellar SH, Sarkar G, Sreekumar R, Bolander ME, Sundt TM 3rd. Elevated expressions of osteopontin and tenascin C in ascending aortic aneurysms are associated with trileaflet aortic valves as compared with bicuspid aortic valves. Cardiovasc Pathol. 2007 May-Jun;16(3):144-50. Epub 2007 Feb 21.

54. Robicsek F. Bicuspid versus tricuspid aortic valves. J Heart Valve Dis. 2003 Jan;12(1):52-3.

55. Parai JL, Masters RG, Walley VM, Stinson WA, Veinot JP. Aortic medial changes associated with bicuspid aortic valve: myth or reality? Can J Cardiol. 1999 Nov;15(11):1233-8.

56. Carè A, Catalucci D, Felicetti F, Bonci D, Addario A, Gallo P, Bang ML, Segnalini P, Gu Y, Dalton ND, Elia L, Latronico MV, Høydal M, Autore C, Russo MA, Dorn GW 2nd, Ellingsen O, Ruiz-Lozano P, Peterson KL, Croce CM, Peschle C, Condorelli G. MicroRNA-133 controls cardiac hypertrophy. Nat Med. 2007 May;13(5):613-8. Epub 2007 Apr 29.

57. Isenberg JS, Roberts DD, Frazier WA. CD47: a new target in cardiovascular therapy. Arterioscler Thromb Vasc Biol. 2008 Apr;28(4):615-21. Epub 2008 Jan 10.

58. Scalbert E, Bril A. Implication of microRNAs in the cardiovascular system. Curr Opin Pharmacol. 2008 Apr;8(2):181-8. Epub 2008 Feb 19.